
This is an electronic reprint of the original article.

This reprint may differ from the original in pagination and typographic detail.

Author(s): Nagase, M. & Lindén, J. & Miettinen, J. & Karppinen, Maarit & Yamauchi, H.

Title: Layered (Cu,Fe) oxides of double perovskite structure: Correlation between structural and magnetic-property changes in BaY(Cu_{0.5}Fe_{0.5})₂O₅+ δ upon high-pressure heat treatment

Year: 1998

Version: Final published version

Please cite the original version:

Nagase, M. & Lindén, J. & Miettinen, J. & Karppinen, Maarit & Yamauchi, H. 1998. Layered (Cu,Fe) oxides of double perovskite structure: Correlation between structural and magnetic-property changes in BaY(Cu_{0.5}Fe_{0.5})₂O₅+ δ upon high-pressure heat treatment. Physical Review B. Volume 58, Issue 6. 3371-3376. ISSN 1550-235X (electronic). DOI: 10.1103/physrevb.58.3371.

Rights: © 1998 American Physical Society (APS). This is the accepted version of the following article: Nagase, M. & Lindén, J. & Miettinen, J. & Karppinen, Maarit & Yamauchi, H. 1998. Layered (Cu,Fe) oxides of double perovskite structure: Correlation between structural and magnetic-property changes in BaY(Cu_{0.5}Fe_{0.5})₂O₅+ δ upon high-pressure heat treatment. Physical Review B. Volume 58, Issue 6. 3371-3376. ISSN 1550-235X (electronic). DOI: 10.1103/physrevb.58.3371, which has been published in final form at <http://journals.aps.org/prb/abstract/10.1103/PhysRevB.58.3371>.

All material supplied via Aaltodoc is protected by copyright and other intellectual property rights, and duplication or sale of all or part of any of the repository collections is not permitted, except that material may be duplicated by you for your research use or educational purposes in electronic or print form. You must obtain permission for any other use. Electronic or print copies may not be offered, whether for sale or otherwise to anyone who is not an authorised user.

Layered (Cu,Fe) oxides of double perovskite structure: Correlation between structural and magnetic-property changes in $\text{BaY}(\text{Cu}_{0.5}\text{Fe}_{0.5})_2\text{O}_{5+\delta}$ upon high-pressure heat treatment

M. Nagase

Materials and Structures Laboratory and Department of Materials Science and Engineering, Interdisciplinary Graduate School, Tokyo Institute of Technology, Yokohama 226-8503, Japan

J. Lindén

Physics Department, Åbo Akademi, FIN-20500 Turku, Finland

J. Miettinen

Department of Technical Physics, Helsinki University of Technology, FIN-02015 Espoo, Finland

M. Karppinen

*Materials and Structures Laboratory, Tokyo Institute of Technology, Yokohama 226-8503, Japan
and Laboratory of Inorganic and Analytical Chemistry, Helsinki University of Technology, FIN-02015 Espoo, Finland*

H. Yamauchi

Materials and Structures Laboratory and Department of Materials Science and Engineering, Interdisciplinary Graduate School, Tokyo Institute of Technology, Yokohama 226-8503, Japan

(Received 3 March 1998)

In this paper, we report the correlation between the magnetic property and the local structure in $\text{BaY}(\text{Cu}_{0.5}\text{Fe}_{0.5})_2\text{O}_{5+\delta}$ of the “0112” phase containing an unusually large amount of excess oxygen, δ of ~ 0.2 , when heat treated under a high pressure of 5 GPa. Magnetic susceptibility measurements showed that upon the high-pressure heat treatment, the lower-temperature magnetic transition which had been observed in normal-pressure synthesized, antiferromagnetic $\text{BaY}(\text{Cu}_{0.5}\text{Fe}_{0.5})_2\text{O}_5$ disappeared and the higher-temperature transition, i.e., the Néel temperature, was lowered. According to a Rietveld analysis based on x-ray-diffraction data and space group $P4/mmm$, the distinction between Cu and Fe positions along the c axis inside the oxygen pyramid disappeared. Coulometric titrations and Mössbauer spectroscopy measurements strongly suggested the existence of excess oxygen in the yttrium plane. [S0163-1829(98)03329-3]

I. INTRODUCTION

The known superconducting cuprate phases expressed by $M_m\text{A}_2\text{Q}_{n-1}\text{Cu}_n\text{O}_{2+m+2n\pm\delta}$ or $M-m2(n-1)n$ consist of alternating superconducting $\text{Q}_{n-1}\text{Cu}_n\text{O}_{2n}$ “infinite-layer” and $M_m\text{O}_{m\pm\delta}$ “charge reservoir” blocks, separated by AO rock-salt layers.¹ The superconductivity transition temperature (T_c) is controlled mainly by tuning the hole-doping level and distribution within the CuO_2 planes in the infinite-layer block,² while tailoring the layered cuprate structures along the vertical axis seems to be more effective in terms of controlling the irreversibility field (H_{irr}) of magnetization.³ Improvements in the H_{irr} characteristics have been achieved by making the $M_m\text{A}_2\text{Q}_{n-1}\text{Cu}_n\text{O}_{2+m+2n\pm\delta}$ structures less anisotropic.⁴ Thorough characterization of layered cuprate structures with $M_m\text{A}_2\text{O}_{2+m\pm\delta}$ charge reservoir blocks as thin as possible is thus highly motivated. In that respect, the importance of searching for and investigating the case of $m=0$ and single AO layer, i.e., the $\text{AQ}_{n-1}\text{Cu}_n\text{O}_{1+2n\pm\delta}$ phases or the members of “01($n-1$) n ” homologous series was recognized.⁵

The so-called “oxygen-deficient double-perovskite” $\text{BaY}(\text{Cu}_{0.5}\text{Fe}_{0.5})_2\text{O}_5$,^{6,7} with barium and yttrium ions ordered along the c axis, can be categorized as an $n=2$ member of

the 01($n-1$) homologous series.⁵ So far this phase has been stabilized only with quite a fixed oxygen content ($\delta \approx 0$) and with at least half occupation of the transition element site by iron or cobalt, i.e., $\text{BaY}(\text{Cu}_{0.5+x}\text{Fe}_{0.5-x})_2\text{O}_5$ ($x=0$),^{6,7} $\text{BaY}(\text{Co}_{1-x}\text{Cu}_x)_2\text{O}_5$ ($0.15 \leq x \leq 0.5$),⁸⁻¹⁰ and $\text{BaY}(\text{Co}_{0.5}\text{Cu}_{0.5-x}\text{Fe}_x)_2\text{O}_5$ ($0.15 \leq x \leq 0.3$).¹¹

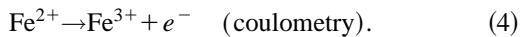
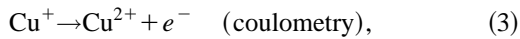
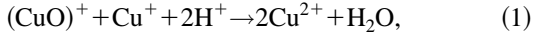
Application of high pressures for the synthesis might, however, promote the stabilization of pure CuO_2 planes [not $(\text{Cu},M)\text{O}_2$ planes with $M=\text{Co},\text{Fe}$] with the required high nominal valence of the transition element site ($+2.5$). Further fine tuning of the Cu valence in terms of satisfying the limitations set by the coordination pyramid (which is characteristic only for divalent copper) is supposed to be achieved, e.g., by a partial La substitution for the Ba site. As a first step of our extensive study on the $(\text{Ba},\text{La})(\text{Y},\text{Ca},\text{La})(\text{Cu},\text{Fe})_2\text{O}_{5+\delta}$ system, the stability of the 0112 phase under high pressure was confirmed and the possible changes upon the high-pressure heat treatment were investigated. The observed changes in the chemical, structural, and magnetic properties of the $\text{BaY}(\text{Cu}_{0.5}\text{Fe}_{0.5})_2\text{O}_{5+\delta}$ phase are reported in the present contribution. For the sample characterization, wet-chemical analysis (for the oxygen content) as well as x-ray diffraction (XRD), TEM, superconducting quantum interference device (SQUID) and ^{57}Fe Möss-

bauer measurements (for the structural and magnetic properties) were employed.

II. EXPERIMENTAL

First, an oxide powder mixture of the nominal cation ratios, $\text{Ba:Y:Cu:Fe}=1:1:1:1$, was prepared from powders of BaCO_3 , Y_2O_3 , Fe_2O_3 , and CuO . For the samples to be studied by Mössbauer spectroscopy, $^{57}\text{Fe}_2\text{O}_3$ (50% ^{57}Fe -enriched) was used instead of the natural Fe_2O_3 . The powder mixture of the starting materials was calcined twice in air at 900°C for 12 h with an intermediate grinding and sintered in air at 1000°C for 24 h (sample A). Then, small portions (~ 100 mg) of sample A powder were separated and tightly packed into gold capsules of 4 mm diameter and 3.7 mm height. Each gold capsule was covered by a NaCl separator and placed into a pyrophyllite container with an internal graphite tube heater. Finally, the high-pressure heat treatment was carried out in a cubic-anvil-type high-pressure apparatus at 5 GPa and 1200°C for 30 min (sample B).

The absolute oxygen contents in samples A and B were determined by a coulometric $\text{Cu}(+I)/\text{Cu}(+II)$ titration method¹² using the experimental setup described elsewhere.¹³ In the present case, the possible trivalent copper and peroxide-type oxygen [Eq. (1)] as well as the trivalent iron [Eq. (2)] are reduced by $\text{Cu}(+I)$ when dissolving the sample in 1 M HCl solution containing a known excess of monovalent copper. On the other hand, if the sample itself contains monovalent copper or divalent iron, less $\text{Cu}(+I)$ is consumed. The oxygen content of the sample can thus be calculated from the coulometric titration result when the resulting sum of $\text{Cu}(+I)$ and $\text{Fe}(+II)$ is determined by anodic oxidation [Eqs. (3) and (4)] as the final analysis step:



The synthesized samples were checked for phase purity by x-ray diffraction. Also, the lattice parameters and the atomic positions were refined in space group $P4/mmm$ from the XRD data using a fitting program, RIETAN. The structures and the cation compositions were confirmed by electron diffraction and high-resolution transmission electron microscopy (Hitachi H-9000) and EDX analysis (Kevex Sigma).

The dc magnetization of the samples was measured under an applied field of 1 T with a SQUID magnetometer (Quantum Design MPMSR) in the temperature range of 5–300 K and with a magnetic balance apparatus using the Faraday method in the temperature range of 300–600 K.

The Mössbauer absorber was prepared by mixing 30 to 50 mg of the sample material with varnish and evenly distributing it on an aluminum foil. The absorber diameter was chosen to achieve an absorber thickness of approximately 22 mg sample per cm^2 . Measurements in transmission geometry were performed with an Amersham $^{57}\text{Co:Rh}$ (20~mCi, January 1995) source. A linear velocity scale with a maximum of 15 mm/s was applied. Measurements were per-

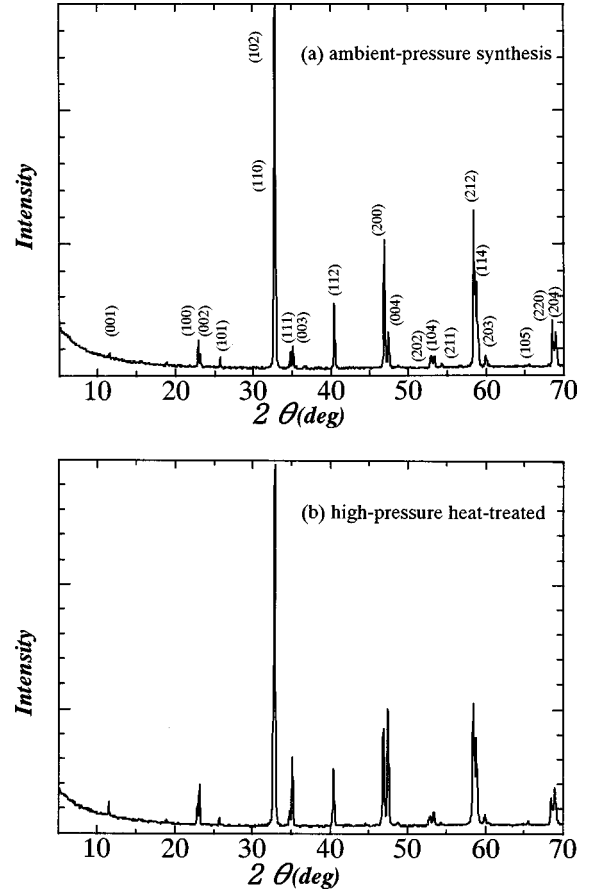


FIG. 1. XRD patterns for $\text{BaY}(\text{Cu}_{0.5}\text{Fe}_{0.5})_2\text{O}_{5+\delta}$ samples (a) synthesized at ambient pressure (sample A) and (b) heat treated at high pressure (sample B).

formed at room temperature and also at 20 K. The spectra were fitted with the Hamiltonian of combined electric and magnetic interactions. The following hyperfine parameters were thus obtained from the fits: the internal magnetic field experienced by the Fe nucleus (B), the chemical isomer shift relative to $\alpha\text{-Fe}$ (Δ), the quadrupole coupling constant (eQV_{zz}), the resonance linewidth, and the relative intensity of each component. The number of possible spectral components was limited to five. Each component corresponds to either a specific lattice site or to a lattice site subjected to a specific chemical environment. Additionally the internal

TABLE I. Refined structure parameters (space group $P4/mmm$) of ambient-pressure synthesized $\text{BaY}(\text{Cu}_{0.5}\text{Fe}_{0.5})_2\text{O}_5$ (sample A). $a = 3.8779(3) \text{ \AA}$, $b = 3.8779(3) \text{ \AA}$, $c = 7.6717(7) \text{ \AA}$, $R_p = 6.70\%$, $R_p = 5.05\%$, $R_e = 2.41\%$.

Atom	x	y	z	$B(\text{\AA}^2)$ or $\beta_{ij} \times 10^4$	Occupancy
Ba	0.0	0.0	0.0	0.85	1
Y	0.0	0.0	0.500 00	0.50	1
Cu	0.5	0.5	0.286 42	0.25	0.5
Fe	0.5	0.5	0.251 40	0.75	0.5
O(1)	0.5	0.5	0.0	0.25	1
O(2)	0.5	0.0	0.314 03	0.75	1
O(3)	0.5	0.0	0.500 00	0.75	0.043

magnetic field was allowed to be distributed over a certain range of values. This was done by assuming a suitable asymmetric distribution.⁷

III. RESULTS AND DISCUSSION

Judging from the x-ray diffraction data, both samples synthesized under ambient pressure (sample A) and heat treated under a high pressure of 5 GPa (sample B) are of single phase as shown in Fig. 1. In high-resolution transmission-electron-micrographs and corresponding electron-diffraction patterns obtained for samples A and B no apparent differences were observed. EDX analyses showed that within the error limits the cation compositions of the two samples were identical.

The structure of $\text{BaY}(\text{Cu}_{0.5}\text{Fe}_{0.5})_2\text{O}_5$ has been discussed in two possible space groups: $P4mm$ allowing two different sites for iron and copper ions^{14,15} and $P4/mmm$ assuming one single Cu/Fe site.⁷ Space group $P4mm$ was suggested by Meyer *et al.*¹⁴ and Pissas *et al.*¹⁵ from Mössbauer spectra of $\text{BaY}(\text{Cu}_{0.5}\text{Fe}_{0.5})_2\text{O}_5$ and $\text{BaR}(\text{Cu}_{0.5}\text{Fe}_{0.5})_2\text{O}_5$ (R =rare-earth element) which displayed only one component with a broad distribution of the hyperfine fields. On the other hand, recently, the Rietveld analysis and Fourier-difference synthesis from powder neutron-diffraction data by Caignaert *et al.*⁷ showed that the $\text{BaY}(\text{Cu}_{0.5}\text{Fe}_{0.5})_2\text{O}_5$ structure was best described in space group $P4/mmm$ with a small splitting of the Cu and Fe positions along the c axis. Therefore, in the present work, a Rietveld refinement for the $\text{BaY}(\text{Cu}_{0.5}\text{Fe}_{0.5})_2\text{O}_5$ sample synthesized at ambient pressure (sample A) was done in the centrosymmetric space group, $P4/mmm$. The refined structural parameters are given in Table I, being in good agreement with Caignaert *et al.*⁷ A Rietveld refinement for the $\text{BaY}(\text{Cu}_{0.5}\text{Fe}_{0.5})_2\text{O}_{5+\delta}$ sample heat treated at high pressure (sample B) was carried out in the same space group, i.e., $P4/mmm$. The refined structural parameters are given in Table II. The refinement converged (with a clear minimum in R_{wp}) into a structure in which the splitting of the Fe/Cu position which had been clearly observed for sample A was negligible for sample B. However, the achieved R_{wp} value (7.75%) remained somewhat larger than that obtained for sample A (6.70%).

In order to determine the contents of excess oxygen in the samples, coulometric titrations were carried out. According to the results of several parallel coulometric titrations, excess oxygen in sample B was $\delta_B = 0.17 \pm 0.01$, while that in sample A was very close to the nominal value, i.e., $\delta_A = 0.03 \pm 0.01$. Also the structure refinements based on the XRD data resulted in a higher oxygen content value for sample B ($\delta_B = 0.078$) than for sample A ($\delta_A = 0.043$). However, the origin of excess oxygen in the high-pressure heat-treated sample (sample B) is not fully understood.

According to a conventional bond-valence-sum¹⁶ calculation, the high-pressure heat treatment with an apparent incorporation of excess oxygen into the structure results in an increase in the valence value of both Cu (from +2.167 to +2.209) and Fe (from +2.789 to +2.901) as can be seen from Tables III and IV. The buckling of the $(\text{Fe}_{0.5}\text{Cu}_{0.5})\text{O}_2$ planes was found to be stronger around Fe (buckling angle 13.9°) than around Cu (buckling angle 6.2°) in sample A. With the high-pressure heat treatment (sample B), the buck-

TABLE II. Refined structure parameters (space group $P4/mmm$) of high-pressure heat treated $\text{BaY}(\text{Cu}_{0.5}\text{Fe}_{0.5})_2\text{O}_{5+\delta}$ (sample B). $a = 3.8796(5)$ Å, $b = 3.8796(5)$ Å, $c = 7.6653(7)$ Å, $R_{wp} = 7.75\%$, $R_p = 5.42\%$, $R_e = 2.01\%$.

Atom	x	y	z	$B(\text{\AA}^2)$ or $\beta_{ij} \times 10^4$	Occupancy
Ba	0.0	0.0	0.0	0.80	1
Y	0.0	0.0	0.500 00	0.25	1
Cu	0.5	0.5	0.271 13	0.70	0.5
Fe	0.5	0.5	0.272 15	0.70	0.5
O(1)	0.5	0.5	0.0	0.25	1
O(2)	0.5	0.0	0.308 24	0.25	1
O(3)	0.5	0.0	0.500 00	0.25	0.078

ling around the Fe atoms significantly reduced (buckling angle 8.1°), the Fe position becoming almost identical to the Cu position (buckling angle 8.3°) (See Table IV).

The results of susceptibility measurements performed for the two samples are shown in Figs. 2(a) and 2(b). For sample A, the $1/\chi$ curve exhibited two magnetic transitions with the following transition temperatures: $T_{N1A} \cong 440$ K and $T_{N2A} \cong 200$ K as shown in Fig. 2(a). Caignaert *et al.*,⁷ also observed two transition temperatures of $T_{N1} \cong 440$ K and $T_{N2} \cong 200$ K by means of the Faraday method using a Cahn RG microbalance and assigned the former to the Néel temperature of a paramagnetic-antiferromagnetic transition and the latter to an incommensurate magnetic transition with a sort of short-range order. On the other hand, the $1/\chi$ curve for sample B exhibits only a single magnetic transition located at $T_{N1B} \cong 340$ K. This Néel temperature (probably for a classical paramagnetic-antiferromagnetic transition) was lower than that for sample A ($T_{N1A} \cong 440$ K). Figure 2(b) shows the $1/\chi$ curve measured for sample B in a magnetic balance apparatus in vacuum as temperature was increased from 300 up to 600 K and then decreased down to 300 K (with heating and cooling rates of 100 °C/h). It was found that upon the heating and cooling cycle, the Néel tempera-

TABLE III. Selected bond lengths (Å) and bond angles/buckling angles (°), and calculated bond-valence sums (BVS) in the ambient-pressure synthesized $\text{BaY}(\text{Cu}_{0.5}\text{Fe}_{0.5})_2\text{O}_5$ (sample A).

Bond	No. × Occupancy	Bond length (Å)	BVS
Y-O(2)	× 8	2.4073(0)	2.825 for Y ion
Y-O(3)	× 4 × 0.043	2.7421(0)	
Ba-O(1)	× 4	2.7421(1)	2.065 for Ba ion
Ba-O(2)	× 8	3.0925(1)	
Cu-O(1)		2.1973(4)	2.167 for Cu ion
Cu-O(2)	× 4	1.9505(0)	
Cu-O(3)	× 0	1.6385(3)	2.789 for Fe ion
Fe-O(1)		1.9286(8)	
Fe-O(2)	× 4	1.9976(1)	
Fe-O(3)	× 2 × 0.043	1.9072(0)	
Bond kink type		Bond angle (°)	Buckling angle (°)
O(2)-Cu-O(2)		167.53(1)	6.24
O(2)-Fe-O(2)		152.16(4)	13.92

TABLE IV. Selected bond lengths (\AA) and bond angles/buckling angles ($^\circ$), and calculated bond-valence sums (BVS) in the high-pressure heat treated $\text{BaY}(\text{Cu}_{0.5}\text{Fe}_{0.5})_2\text{O}_{5+\delta}$ (sample *B*).

Bond	No. \times Occupancy	Bond length (\AA)	BVS
Y-O(2)	$\times 8$	2.4338(2)	2.651 for Y ion
Y-O(3)	$\times 4 \times 0.078$	2.7433(2)	
Ba-O(1)	$\times 4$	2.7433(2)	2.152 for Ba ion
Ba-O(2)	$\times 8$	3.0570(4)	
Cu-O(1)		2.0782(9)	2.209 for Cu ion
Cu-O(2)	$\times 4$	1.9605(7)	
Cu-O(3)	$\times 0$	1.7543(5)	
Fe-O(1)		2.0861(1)	2.901 for Fe ion
Fe-O(2)	$\times 4$	1.9594(5)	
Fe-O(3)	$\times 2 \times 0.078$	1.7465(3)	
Bond kink type		Bond angle ($^\circ$)	Buckling angle ($^\circ$)
O(2)-Cu-O(2)		163.31(5)	8.35
O(2)-Fe-O(2)		163.76(5)	8.12

ture, T_{N1B} of sample *B* increased while that of sample *A* remained unchanged. This different behavior is probably due to the observed difference in the excess oxygen content in the two samples: during the heating and cooling cycle in

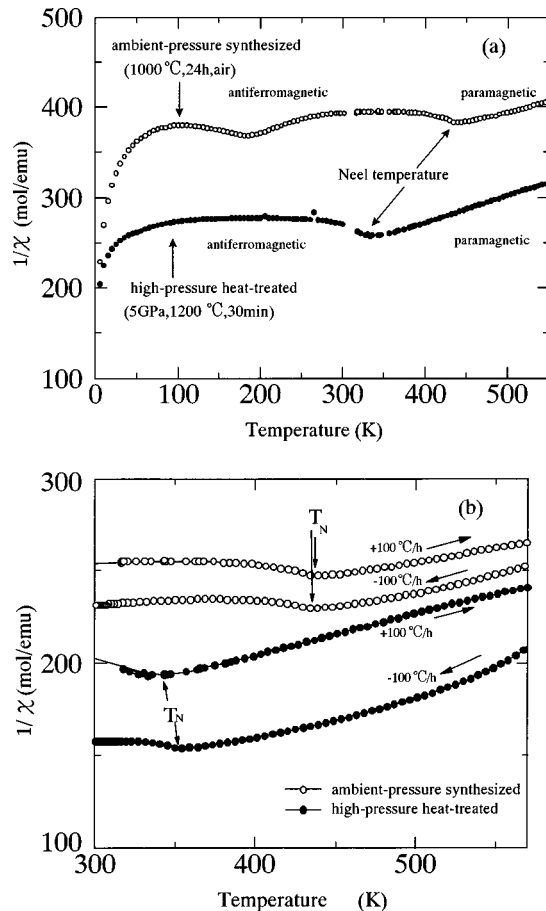


FIG. 2. Reciprocal molar magnetic susceptibility vs temperature for $\text{BaY}(\text{Cu}_{0.5}\text{Fe}_{0.5})_2\text{O}_{5+\delta}$ samples (a) at 5–600 K and (b) at 300–600 K.

vacuum, excess oxygen in sample *B* was partly released, i.e., lost, and thus the change in the oxygen content seems to affect the value of T_{N1B} .

According to Caignaert *et al.*,⁷ the iron moments at 4 K are not oriented along the crystallographic axes and the tilt of iron moment is probably related to the existence of the incommensurate transition at T_{N2A} . If this incommensurate transition is related to the difference between the Fe and Cu positions, high-pressure heat-treated $\text{BaY}(\text{Cu}_{0.5}\text{Fe}_{0.5})_2\text{O}_{5+\delta}$ in which Fe and Cu occupy identical positions should not show this behavior [cf. Fig. 2(a)]. The reason for Fe atoms to shift towards the Cu position could be the excess O^{2-} ion which attracts the Fe^{3+} ions. The disappearance of the incommensurate magnetic transition that was speculated to be caused by the variation in the Fe and Cu positions could be clarified by performing structural refinement using neutron-diffraction data.

The Mössbauer spectra were recorded at 300 K for both samples [Figs. 3(a) and 3(b)], and also at 20 K for sample *B* [Fig. 3(c)]. All of the three spectra consist of the same four components (as shown in Table V), but the relative intensities of the components are different for the two samples. Component 1, as previously discussed by Caignaert *et al.*,⁷ is a sextet arising from $\text{Fe}(+III)$ with a pyramidal oxygen coordination. Component 2, a sextet too, is assigned to $\text{Fe}(+III)$ with an octahedral oxygen coordination since the quadrupole splitting is very close to zero, i.e., the electric

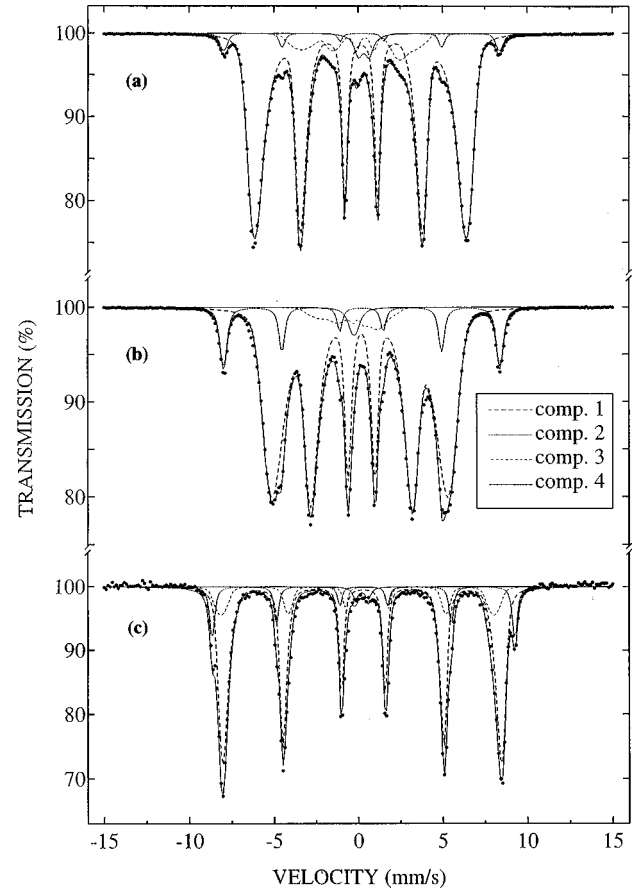


FIG. 3. The Mössbauer spectra recorded at 300 K for $\text{BaY}(\text{Cu}_{0.5}\text{Fe}_{0.5})_2\text{O}_{5+\delta}$ samples (a) synthesized at ambient pressure (sample *A*) and (b) heat treated at high pressure (sample *B*), and (c) the one recorded at 20 K for sample *B*.

TABLE V. Mössbauer results (300 and 20 K) for the $\text{BaYCu}^{57}\text{FeO}_{5+\delta}$ samples. Component 1: square pyramidal Fe(+3), component 2: octahedral Fe(+3), component 3: square pyramidal Fe(+3), component 4: paramagnetic impurity or artifact of fitting.

	Component	Intensity (%)	Field (T)	Quadrupole coupling (mm/s)	Isomer shift relative to α iron (mm/s)
Sample A: normal-pressure synthesized (at 300 K)	1	84.3	39.2 ^a	−0.12	0.255
	2	3.7	50.6	−0.04	0.314
	3	9.0	20.3 ^a	−1.01	0.259
	4	3.0		1.27	0.44
Sample B: high-pressure heat treated (at 300 K)	1	82.7	32.6 ^a	−0.21	0.251
	2	10.2	50.8	−0.02	0.307
	3	5.2	11.1 ^a	−0.85	−0.07
	4	1.9		0.54	−0.13
Sample B: high-pressure heat treated (at 20 K)	1&3	85.7	51.1	−0.33	0.352
	2	12.4	55.5	−0.05	0.356
	4	1.8		1.5	0.33

^aMaximum value.

field is very symmetric. Even though the coordination octahedron of iron with extra oxygen in site O(3) (as defined in Fig. 4) is not quite regular, (as it should be in order to make the quadrupole coupling constant zero) the Fe-O(1) length is elongated, while the Fe-O(3) length becomes pretty short as shown in Table IV. Therefore the net effect is still the same as for a regular octahedron. Only in the case where both lengths were elongated/shortened, would the quadrupole coupling be substantial. In order to confirm the assignment of component 2 to the octahedral oxygen coordination, a portion of sample B powder was additionally post-annealed in Ar gas at 500 °C where the oxygen was supposed to be released from the structure. The Mössbauer spectrum measured for sample B at 300 K after post annealing was identical to the one for sample A, i.e., the intensity of component 2 was lower than that for sample B. Components 1 and 2 together cover more than 88% of the intensity of spectra. Component 3 is probably related to component 1 and merely reflects the various environments of the Fe/Cu sites originating from the random occupation of the Fe and Cu atoms in the same site. In other words, component 3 forms the tail of the distribution of hyperfine parameters observed at the pyramidal site. Component 4 might be an iron-containing impurity or a small discrepancy in the model used for the Fe/Cu distribution. The intensity ratio between components 2 and 1 is larger in sample B than in sample A. This fact strongly indicates that upon the high-pressure heat treatment, the excess oxygen entered the yttrium plane and consequently the coordination environment of the Fe atoms in $\text{BaY}(\text{Cu}_{0.5}\text{Fe}_{0.5})_2\text{O}_{5+\delta}$ increases the coordination number of Fe from five to six. At 20 K components 1 and 3 were no longer very well distinguishable, which supports assigning them to the same oxygen coordination. As seen in Table V, the intensity of component 2 increased slightly, but this is probably a consequence of the fact that at 20 K components 1 and 2 overlap more strongly as both have an internal field stronger than 50 T. As the intensity of component 4 remains

constant, the presence of a paramagnetic impurity is most probable. The internal fields and the isomer shift values clearly indicate that the Fe atom possesses the high spin ($S = 5/2$) trivalent state.

Since both the coulometric titration and Mössbauer results indicated the presence of excess oxygen in sample B, i.e., the high-pressure heat treated one, additional annealing experiments were carried out for sample A which was ambient-pressure synthesized. With annealings performed in both air and argon atmosphere of 1 atm, no changes in oxygen content were resulted, as judged from subsequent coulometric and Mössbauer measurements. Therefore, it could be concluded that the change in both oxygen content and magnetic

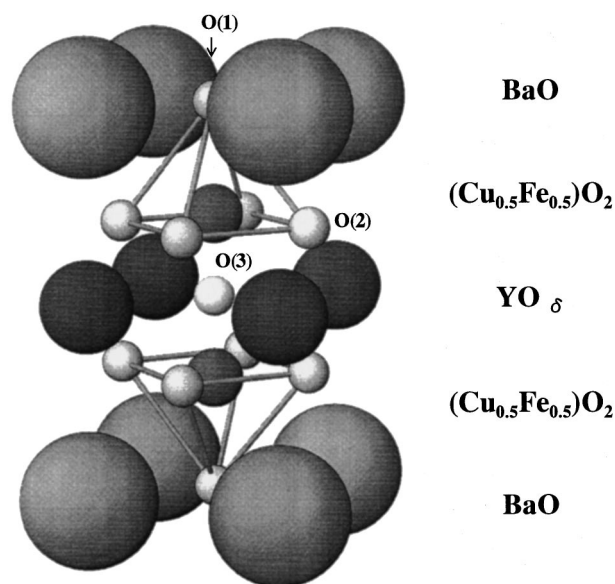


FIG. 4. Schematic presentation of the “0112” structure of $\text{BaY}(\text{Cu}_{0.5}\text{Fe}_{0.5})_2\text{O}_{5+\delta}$ with the employed notation system for the three types of oxygen.

property can be assigned exclusively to the effect of the high-pressure heat treatment.

IV. CONCLUSION

This study showed the correlation between the magnetic property and local structure of a “0112” compound, $\text{BaY}(\text{Cu}_{0.5}\text{Fe}_{0.5})_2\text{O}_{5+\delta}$, heat treated under a high pressure. With the high-pressure heat treatment at 5 GPa and 1200 °C the Néel temperature of an antiferromagnetic transition decreased and the magnetic transition caused by incommensuration with a sort of short-range order disappeared. The decrease in the Néel temperature was likely caused by an uptake of excess oxygen, and the latter transition was sup-

pressed since the Fe atoms shifted towards the Cu site. These changes were realized only by high-pressure heat treatment.

ACKNOWLEDGMENTS

The authors are grateful to Professor M. Itoh and Dr. H. Suematsu of the Tokyo Institute of Technology for their helpful discussions. This work was partially supported by a Grant-in-Aid for Scientific Research under Contract No. 08044135 from The Ministry of Education, Science and Culture of Japan, and also by an International Collaborative Research Project Grant-1997 of the Materials and Structures Laboratory, Tokyo Institute of Technology.

-
- ¹H. Yamauchi, M. Karppinen, and S. Tanaka, *Physica C* **263**, 80 (1996).
- ²H. Yamauchi and M. Karppinen, in *Advances in Superconductivity*, edited by S. Nakajima and M. Murakami (Springer-Verlag, Tokyo, 1997), Vol. IX, pp. 381–386.
- ³H. Yamauchi, M. Karppinen, K. Fujinami, T. Ito, H. Suematsu, H. Sakata, K. Matsuura, and K. Isawa, *Supercond. Sci. Technol.* (to be published).
- ⁴K. Kishio, J. Shimoyama, T. Kimura, Y. Kotaka, K. Kitazawa, K. Yamafuji, Q. Li, and M. Suenaga, *Physica C* **235-240**, 2775 (1994).
- ⁵H. Yamauchi, and M. Karppinen, *Superlattices Microstruct.* **21**, 127 (1997).
- ⁶L. Er-Rakho, C. Michel, Ph. Lacorre, and B. Raveau, *J. Solid State Chem.* **73**, 531 (1988).
- ⁷V. Caignaert, I. Mirebeau, F. Bourée, N. Nguyen, A. Ducouret, J. M. Greneche, and B. Raveau, *J. Solid State Chem.* **114**, 24 (1995).
- ⁸L. Barbey, N. Nguyen, V. Caignaert, M. Hervieu, and B. Raveau, *Mater. Res. Bull.* **27**, 295 (1992).
- ⁹L. Barbey, N. Nguyen, V. Caignaert, F. Studer, and B. Raveau, *J. Solid State Chem.* **112**, 148 (1995).
- ¹⁰Q. Huang, P. Karen, V. L. Karen, A. Kjekshus, J. W. Lynn, A. D. Mighell, I. Natali Sora, N. Rosov, and A. Santoro, *J. Solid State Chem.* **108**, 80 (1995).
- ¹¹L. Barbey, N. Nguyen, A. Ducouret, V. Caignaert, J. M. Greneche, and B. Raveau, *J. Solid State Chem.* **115**, 514 (1995).
- ¹²M. Karppinen, A. Fukuoka, L. Niinistö, and H. Yamauchi, *Supercond. Sci. Technol.* **9**, 121 (1996).
- ¹³K. Kurusu, H. Takami, and K. Shintomi, *Analyst (Cambridge, U.K.)* **114**, 1341 (1989).
- ¹⁴C. Meyer, F. Hartman-Boutron, Y. Gros, and P. Strobel, *Solid State Commun.* **76**, 163 (1990).
- ¹⁵M. Pissas, C. Mitros, G. Kallias, V. Psycharis, A. Simopoulos, A. Kostikas, and D. Niarchos, *Physica C* **192**, 35 (1990).
- ¹⁶I. D. Brown and D. Altermatt, *Acta Crystallogr., Sect. B: Struct. Sci.* **41**, 224 (1985).